

Bioinspired Superhydrophobic Ni–Ti Archwires with Resistance to Bacterial Adhesion and Nickel Ion Release

Ruoxi Liu, Xi Liu, Jie Zhou, Qiong Nie,* Jingxin Meng,* Jiuxiang Lin, and Shutao Wang*

Although orthodontic archwires are made from biomedical materials with vast potential for applications worldwide, great challenges, including the adhesion of cariogenic bacteria, the release of nickel ions, and the weakness of mechanical strength, remain and affect their biocompatibility and service life. Herein, a bioinspired superhydrophobic nickel–titanium alloy archwire is reported that displays multifunctional properties of antibacteria adhesion, antinickel release, and corrosion resistance. Compared with commercially purchased archwires, these performances on superhydrophobic archwires can be significantly elevated by varying the contact mode between archwires and the bacterial suspension from surface contact to point contact. Thus, this bioinspired superhydrophobic design has the potential to be applied in other dental devices and provides new ideas for developing novel multifunctional biomaterials.

1. Introduction

Biomaterials have been extensively applied in the fields of diagnostics,^[1] tissue engineering,^[2] and transplantation,^[3] as well as wound healing.^[4] Nickel–titanium (Ni–Ti) alloy, as one of the most promising biomaterials, has attracted wide attention due to its distinctive properties, such as superelasticity and biocompatibility.^[5] Especially in orthodontic treatment, Ni–Ti alloy has been well received by orthodontists as orthodontic archwires (AWs). However, during clinical treatment with these AWs, the complex microenvironment of the oral cavity, which contains electrolytes, proteins, and bacteria, commonly raises some severe problems, such as the risk of bacterial adhesion,

the corrosion-induced release of nickel ions, and a weakness in the mechanical strength,^[6] thereby leading to the decay of teeth, a nickel allergy in supersensitive individuals,^[7] and a reduction in service efficiency.

To solve these problems, many antibacterial strategies have been developed including anti-adhesive coatings (such as PEG,^[8] zwitterionic polymers,^[9] enzymes,^[10] and other proteins^[11]), bactericidal coatings (such as quaternary ammonium,^[12] Ag ion,^[13] chitosan,^[14] polypeptides,^[15] and surface topographies^[16]), and their combinations (such as smart-responsive surfaces^[17]). In addition, several strategies have been employed to initially solve the nickel-release problem, for instance, oxidation,^[18] surface coating,^[19] and laser treatment,^[20] as well

as ion implantation.^[21] However, the corresponding mechanical properties are probably reduced after the treatments mentioned above.^[22] Therefore, designing multifunctional Ni–Ti archwires by integrating these advantages together remains a great challenge.

Superhydrophobicity is a well-known phenomenon that can be widely observed in nature, such as on a lotus leaf, mosquito eye, and cicada wing.^[23] Because of its abilities, superhydrophobicity is now harnessed in many applications, including anti-icing,^[24] antifogging,^[25] water–oil separation,^[26] and what we are most concerned about—anti-biofouling.^[27] Actually, the self-cleaning property of the lotus leaf owes to the air layer at the interface of the liquid and substrate materials, blocking any interaction between them. Thus, we speculate that the bioinspired superhydrophobic surface may exhibit multifunctional properties, such as antibacteria adhesion and antinickel leakage by reducing the contact area between AWs and bacterial suspensions.

Herein, inspired by the self-cleaning phenomenon of the lotus leaf, we demonstrated a superhydrophobic multifunctional Ni–Ti alloy archwire which combines antibacteria and antinickel release properties (**Figure 1**). Compared with commercially purchased AWs, this superhydrophobic surface not only significantly reduces bacterial adhesion but also suppresses Ni ion release because trapped air on the superhydrophobic surface greatly reduces the contact area between the AWs and bacterial suspension from the surface contact to point contact. In addition, the inherent mechanical properties of the AWs are maintained. Therefore, this strategy provides ideas for the design of new kinds of orthodontic appliances and devices with multifunctional properties.

Dr. R. Liu, Dr. J. Zhou, Prof. Q. Nie, Prof. J. Lin
Department of Orthodontics
Peking University School and Hospital of Stomatology
Beijing 100081, P. R. China
E-mail: nieqiong@bjmu.edu.cn

Dr. X. Liu, Prof. J. Meng, Prof. S. Wang
CAS Key Laboratory of Bio-inspired Materials and Interfacial Science
CAS Center for Excellence in Nanoscience
Technical Institute of Physics and Chemistry
Chinese Academy of Sciences
Beijing 100190, P. R. China
E-mail: mengjx628@mail.ipc.ac.cn; stwang@mail.ipc.ac.cn

Dr. X. Liu, Prof. J. Meng, Prof. S. Wang
University of Chinese Academy of Sciences
Beijing 100049, P. R. China

 The ORCID identification number(s) for the author(s) of this article can be found under <https://doi.org/10.1002/admi.201801569>.

DOI: 10.1002/admi.201801569

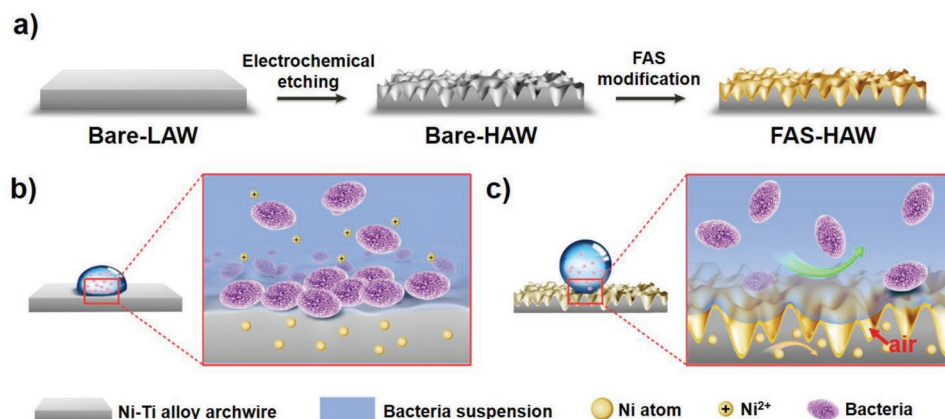


Figure 1. Schematic illustration of anti-adhesion and anti-Ni release behavior on the FAS modified rough orthodontic AWs. a) The modification process of superhydrophobic AWs. Bacteria adhesion and Ni^{2+} release properties of commercially purchased AWs with low roughness (Bare-LAW) for b) and superhydrophobic AWs with high roughness (FAS-HAW) for c).

2. Results and Discussion

2.1. Fabrication of the Superhydrophobic Archwires

The fabrication process of hydrophobic AWs is schematically shown in Figure 1a. First, the AWs were electrochemically etched at 3.0 V in 1 mol L⁻¹ HNO₃ aqueous solution for different times (i.e., 0, 10, and 120 s) to obtain different roughness. In this process, the Ni was gradually dissolved, whereas the Ti was oxidized to form a TiO₂ nanolayer on the surface of the Ni–Ti alloy.^[27b] Scanning electron microscope (SEM) images in Figure 2a and laser scanning confocal microscopy (LSCM) images of Figure S1 in the Supporting Information both show that the roughness of the AWs gradually increases with the prolonged etching time, that is, 0 s for commercially purchased AW with low roughness (LAW), 10 s for AW with moderate roughness (MAW), and 120 s for AW with high roughness (HAW). Furthermore, unaltered LAWs (Bare-LAWs) served as controls. Afterward, 1H, 1H, 2H, 2H-perfluorodecyltrimethoxysilane (FAS) was deposited on the prepared AWs in a decompression environment at 80 °C overnight, as described in previous reports.^[11b] Compared to Bare AWs, the newly appeared peak of fluorine (688 eV) on the X-ray photoelectron spectroscopy (XPS) spectrum (Figure 2d) of the FAS-modified AWs (FAS-AWs) demonstrates the successful deposition of the FAS molecule. Figure 2b displays the wettability of water droplets on the surface of all AWs, showing that the water contact angles (CAs) increase after FAS modification. As shown in Figure 2b, water CA on the Bare-LAWs is found to be 89.5 ± 5.9°, which increases to 122.2 ± 1.6° for FAS-LAW, 137.2 ± 5.1° for FAS-MAW, and 160.4 ± 6.0° for FAS-HAW after FAS modification. In addition, the adhesive forces of water for the abovementioned AWs were investigated as well. Figure 2c shows the curves of adhesive forces and the corresponding images of water droplets on the AW surfaces. When leaving the AW surfaces, the water droplets on Bare-LAW, FAS-LAW, and FAS-MAW are all stretched to some extent and exhibit relative strong water adhesion, demonstrated by the forces of 145.2 ± 14.9, 80.3 ± 4.3, and 49.7 ± 9.6 μN, respectively. In contrast, the water droplet on FAS-HAW maintains its nearly spherical shape, and no residual

water is observed on the AW, which is in accordance with the extremely low adhesive force of 19.4 ± 4.5 μN. Thus, the variation of the CAs and adhesion forces of the modified AWs demonstrate the successful fabrication of the desired surfaces.

2.2. Antibacteria Adhesion Performance

Orthodontic AWs are well known to raise the difficulty of teeth cleaning and enlarge adhesion sites for oral bacteria such as *Streptococcus mutans* (*S. mutans*),^[11b] which readily lead to dental decay. Thus, improving the antibacteria adhesion property of AWs is very important. The bacterial adhesion experiment was operated via incubations of all AWs with *S. mutans* suspensions at a concentration of 1 × 10⁸ cells mL⁻¹ in phosphate-buffered saline (PBS) for different times (i.e., 0, 5, 10, 15, and 20 h).^[11b] To mimic the daily behavior of mouth rinsing, the AWs were removed and gently rinsed in deionized water every 5 h for the duration of the culture time. The number of adhered bacteria was quantified using corresponding SEM images. As shown in Figure S2a (Supporting Information), few bacteria are observed on the FAS-HAWs, which also exhibit an extremely low bacteria adhesion regardless of the incubation time (Figure 3a). In contrast, many bacteria adhere to the Bare-LAW surface (Figure S2d, Supporting Information), exhibiting an apparent increment with the increase of incubation time (Figure 3b). Taking incubation time of 20 h as an example, the density of adhered bacteria is (0.12 ± 0.10) × 10⁴ cm⁻² for FAS-HAW. In contrast, the density is significantly increased to (3.46 ± 0.75) × 10⁴ cm⁻² on the original AW (Bare-LAW), suggesting an excellent antibacterial performance of FAS-HAW, at an efficiency of 96.6%. In addition, the densities of the adhered bacteria in Figure S3a (Supporting Information) are (1.21 ± 0.25) × 10⁴ cm⁻² for FAS-LAW and (0.45 ± 0.20) × 10⁴ cm⁻² for FAS-MAW, displaying an antibacteria efficiency of 65.0% and 87.0%, respectively. Figure S4 (Supporting Information) shows that the bacterial experiment without removal for rinsing exhibits the same trend of bacterial adhesion as observed with removal with rinsing every 5 h. Therefore, these results confirm that the FAS-treated AWs show excellent antibacteria properties.

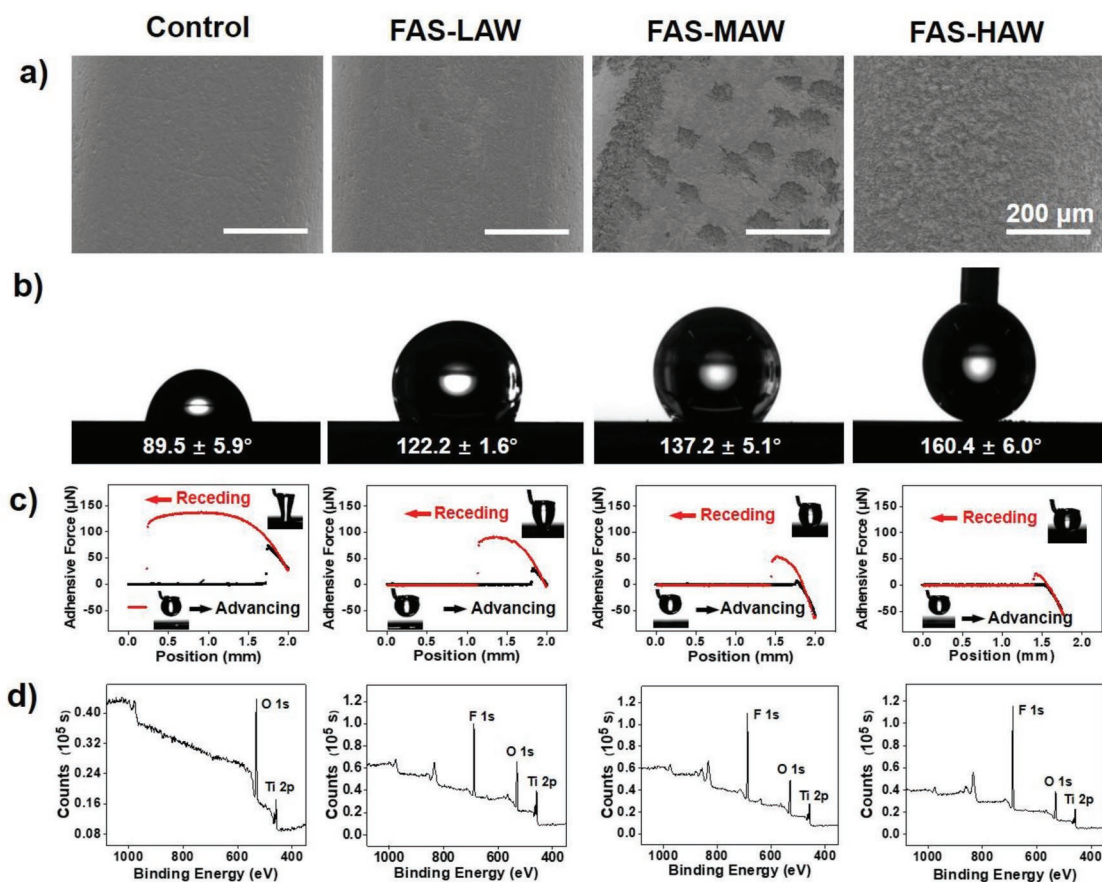


Figure 2. Surface morphology, wettability, adhesion property, and element analysis of Bare-LAW (labeled as Control) and FAS-AWs. a) AW morphologies with different roughness are shown by SEM topographies. b) Contact angles (CAs) of all AWs: Control shows hydrophilicity with CA of $89.5 \pm 5.9^\circ$, and FAS-LAW and FAS-MAW show hydrophobicity with CAs of $122.2 \pm 1.6^\circ$ and $137.2 \pm 5.1^\circ$, respectively, whereas FAS-HAW shows superhydrophobicity, and the CA is $160.4 \pm 6.0^\circ$. c) Adhesive forces of all AWs decrease from $145.23 \pm 14.93 \mu\text{N}$ for Control to $19.40 \pm 4.50 \mu\text{N}$ for FAS-HAW. d) Fluorine peak (688 eV) in XPS spectrum of AWs. Scale bar 200 μm . The error bar represents the standard error from three repeats.

As shown in Figure 3c, only a few bacteria, which are indicated with the red arrow, are found on the surface of the FAS-HAW after a short incubation time (e.g., 0.5 h). In contrast, an apparent bacterial aggregation, indicated by the red dotted line, is clearly observed on the original AW, indicating the initial formation of bacterial biofilm (Figure 3d). In addition, the CAs of all AWs were measured every 5 h when incubated in the bacterial suspension. The results in Figure 3a,b and Figure S3b (Supporting Information) show that no obvious CA variation exists in the AWs, demonstrating the stability of surface wettability and corresponding antibacteria.

2.3. Anti-Ni Ion Release Property and Corrosion Resistance

Since superfluous Ni ion in the oral environment probably leads to allergy and cytotoxicity, enhancing the anti-Ni release of the Ni-Ti alloy AWs is essential. Therefore, we compared the anti-Ni release property of the different AWs including the Bare-LAW, FAS-LAW, Bare-HAW, and FAS-HAW. In brief, we first placed these AWs into a bacterial suspension for 5 h. Then, we monitored the Ni²⁺ concentration of the residual liquid using

inductively coupled plasma mass spectrometry (ICP-MS) after removing the bacteria and AWs. The results in Figure 4b show that the release concentration of Ni²⁺ for FAS-LAW ($8.00 \pm 0.59 \text{ ng mL}^{-1}$) is slightly lower than that shown in Figure 4a for Bare-LAW ($8.33 \pm 0.71 \text{ ng mL}^{-1}$), which may stem from the wettability transition from hydrophilicity to hydrophobicity after FAS modification. Compared to that of Bare-LAW in Figure 4a, Bare-HAW in Figure 4c displays an apparent increase of Ni²⁺ concentration to $83.07 \pm 6.59 \text{ ng mL}^{-1}$, owing to enlarged contact area between bacteria suspension and AWs from the amplification of surface roughness (Figure 2a and Figure S1, Supporting Information). Furthermore, the Ni²⁺ concentration for superhydrophobic FAS-HAW in Figure 4d dramatically decreases to $3.64 \pm 0.13 \text{ ng mL}^{-1}$ because trapped air triggers the variation of suspension-AW contact mode from surface contact to point contact. Compared to that of Bare-LAW and Bare-HAW, the Ni²⁺ release of as-prepared FAS-HAW is greatly decreased by 56.3% and 95.6%, indicating that FAS-HAW possesses an excellent performance of anti-Ni release. Therefore, the potential allergy risk can be greatly alleviated by reducing the actual contact area between the bacterial suspension and the AWs through surface roughening and hydrophobic modification.

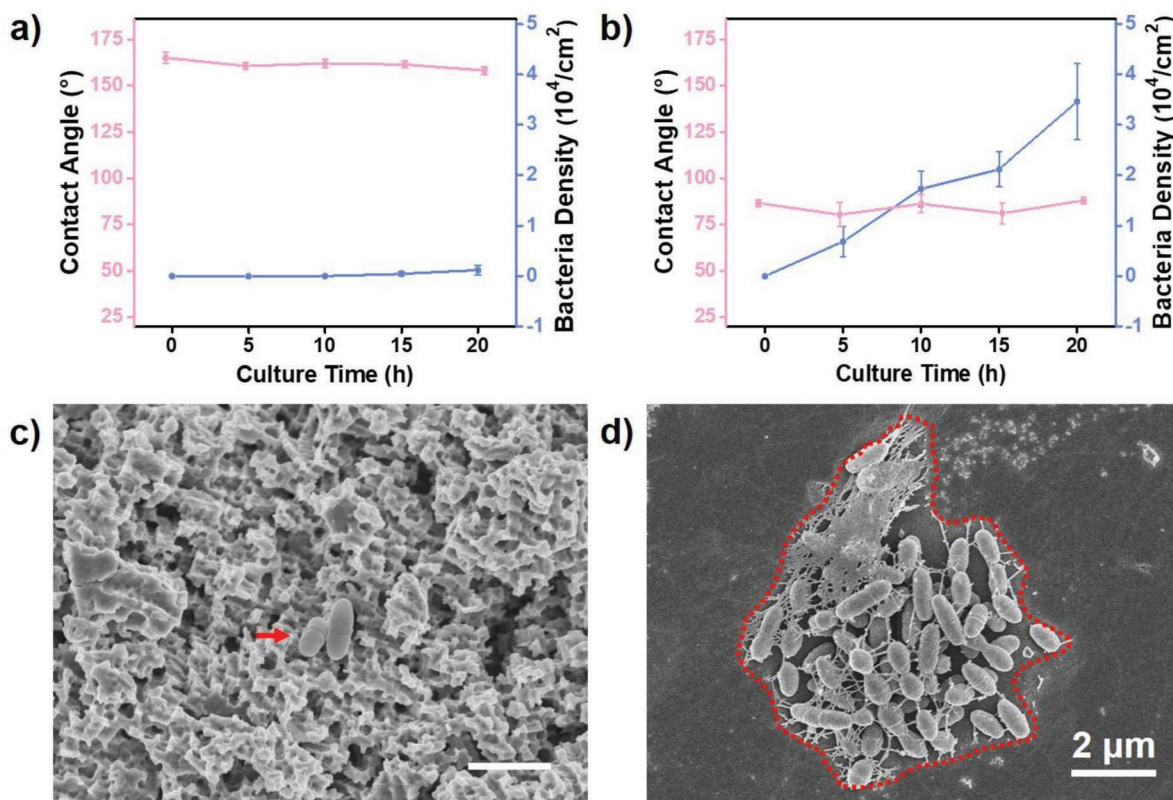


Figure 3. The bacteria adhesion performance and CA variations of Bare-LAW and FAS-HAW when incubated with a bacterial suspension for different time. Bacteria densities (showed by blue lines) and CAs (shown by pink lines) of superhydrophobic FAS-HAW a) and Bare-LAW b). c) Few bacteria can be found on the FAS-HAW, indicated by the red arrow, where no biofilm formation is observed. d) An obvious bacteria aggregation occurs on Bare-LAW when incubated for 0.5 h, as indicated by the red dotted line.

Generally, chemical and electrochemical corrosion of the AWs is inevitable because the oral cavity is a complex environment with electrolytes and metallic dental restorations. To verify their anticorrosion capability, the corrosion current density of different AWs was compared in Figure S5 (Supporting Information). The results show that for Bare-AWs of the black line, the corrosion current density increases from $(2.88 \pm 0.09) \times 10^{-8} \text{ A cm}^{-2}$ (Bare-LAW) to $(39.44 \pm 9.26) \times 10^{-8} \text{ A cm}^{-2}$ (Bare-HAW), with the increase in surface roughness. For the red line of FAS-AWs, compared to $(2.16 \pm 0.12) \times 10^{-8} \text{ A cm}^{-2}$ for FAS-LAW, the corrosion current density for FAS-MAW slightly rises to $(2.22 \pm 0.07) \times 10^{-8} \text{ A cm}^{-2}$, followed by a sharp decline to $(0.90 \pm 0.03) \times 10^{-8} \text{ A cm}^{-2}$ for FAS-HAW. To explain the slight increase of corrosion current density from FAS-LAW to FAS-MAW, their wetting states must be determined. The larger adhesive forces (80.3 ± 4.27 and $49.7 \pm 9.6 \mu\text{N}$) in Figure 2c indicate the hydrophobic Wenzel states of FAS-LAW and FAS-MAW. Compared with FAS-LAW, the rougher FAS-MAW enlarges the actual contact area between the rough AWs and the bacterial suspension, resulting in the slight increase in corrosion current density. Compared to that of Bare-LAW and Bare-HAW, superhydrophobic FAS-HAW is able to promote the corrosion resistance of AWs up to 68.7% and 97.7%. As a result, the superhydrophobic AWs also exhibit excellent corrosion resistance.

2.4. Mechanical Properties of As-Prepared AWs

Flexural strength, one of the most important mechanical characteristics of orthodontic AWs, was investigated in a three-point bending test.^[28] All AWs were tested according to ISO/CD 15841:2004, MOD standard, and stress–strain curves were drawn to visualize the flexural properties. Figure S6 (Supporting Information) shows that the unloading curves generally overlapped, and the unloading force shows no significant difference, with the compression deformation varying from 3 to 0.5 mm, revealing that the original flexural property is retained. That is, FAS-AWs provide harmless force to teeth when used in orthodontic treatment.

3. Conclusion

In conclusion, we have developed a bioinspired superhydrophobic strategy endowing Ni–Ti alloy AWs with multifunctional properties, including antibacteria adhesion, anti-Ni ion release, and corrosion resistance. These integrated properties attribute to the trapped air on the superhydrophobic surface, significantly reducing the actual contact area between the rough AWs and the

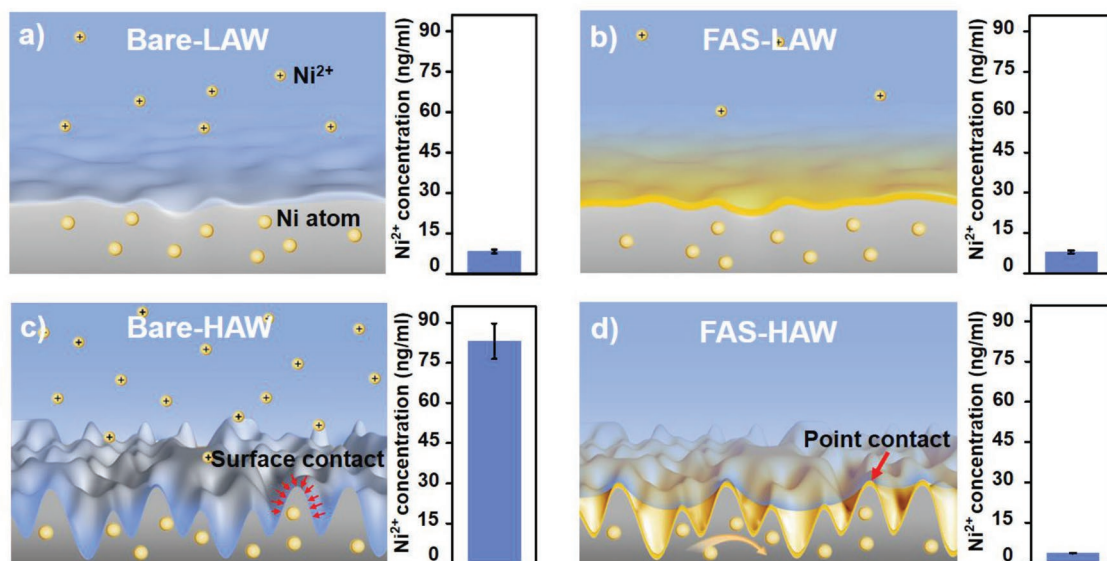


Figure 4. Schematic illustration of anti-Ni release property and corresponding Ni^{2+} concentration of different AWs including Bare-LAW a), FAS-LAW b), Bare-HAW c), and FAS-HAW d). The amount of Ni ion release is mainly related to the contact area between the AWs and the bacterial suspension. With the combination of rough surface and FAS modification, the superhydrophobic FAS-HAW is obtained, significantly decreasing the actual contact area due to the trapped air, thereby resulting in the suppression of Ni ion release.

bacterial suspension. Therefore, our design strategy has potential for application in other dental devices and biomaterials.

4. Experimental Section

Material and Methods: Nickel–Titanium orthodontic archwires were purchased from Smart Co., China. Brain heart infusion and brain heart infusion agar were obtained from Oxoid Co., England. Phosphate-buffered saline was purchased from Thermo Scientific, USA. Acetone (>99.5%, AR) and alcohol ($\geq 99.8\%$, GR) were obtained from the Beijing Chemical Co., China. 1H, 1H, 2H, 2H-Perfluorodecyltrimethoxysilane was bought from J&K Chemical, China. Deionized water (>1.82 M Ω cm, Milli-Q system) was used. All chemicals were used directly without further modification.

Apparatus and Characterization: SEM images were recorded using an S-4800 instrument (HITACHI, Japan). Static contact angles were measured on a Dataphysics OCA 20 Contact-Angle System (Filderstadt, Germany), and the adhesive force was measured using Dataphysics DCAT 21 Dynamic Contact Angle Meter (FILDERSTADT, Germany). The elemental analysis was conducted by X-ray photoelectron spectroscopy (ESCALAB 250XI, Thermo Fisher Scientific, USA). LSCM images with an area of $1 \mu\text{m} \times 1 \mu\text{m}$ were tested by employing Olympus LEXT Nano Search Microscope (OLS4500, Japan). The nickel ion concentration was measured using ICP-MS (X II, Thermo Fisher Scientific, USA).

Bacterial Culture: *S. mutans* (UA159) was used as the model bacteria because it was the dominant bacteria inducing dental decay.^[29] For *S. mutans*, a single bead was taken from its freezing solution in -80°C and incubated for 48 h on brain heart infusion agar at 37°C in an atmosphere enriched with 5% CO_2 . Then, one colony was isolated from the agar and incubated with 1 mL of nutrient broth overnight at 37°C in an atmosphere enriched with 5% CO_2 . After reaching the logarithmic phase, *S. mutans* was harvested by centrifugation at 2000 rpm for 10 min at room temperature and washed with PBS three times. Subsequently, the bacteria were suspended in PBS at a final concentration of 1×10^8 colony-forming units (CFU) mL^{-1} .^[11b]

Fabrication of AWs Modified by FAS: To remove surface organic contamination, AWs were first ultrasonicated in acetone, ethanol, and deionized water for 30, 30, and 30 min, respectively. Then, for

regulated surface roughness, AWs were electrochemically etched in diluted nitric acid (1 mol L^{-1}) at a voltage of 3 V for different times including 0 s (bare AWs with low roughness, Bare-LAW, labeled as Control), 10 s (bare AWs with moderate roughness, Bare-MAW), and 120 s (bare AWs with high roughness, Bare-HAW). Later, the FAS was successfully modified on AWs by the vapor deposition method (decompression environment, 80°C , overnight). Finally, these materials were adequately washed with deionized water three times and dried with N_2 flow, obtaining FAS-modified AWs with different surface roughness (e.g., FAS-LAW, FAS-MAW, and FAS-HAW).

Anti-Adhesion Performance of AWs: To test the anti-adhesion performance, Bare-LAWs (Control) and FAS-AWs were immersed in bacteria suspensions for 5, 10, 15 and 20 h at 37°C . Furthermore, to mimic the daily behavior of mouth rinsing, all AWs were taken out and gently rinsed in deionized water and returned to the bacterial suspension every 5 h for the duration of the total culture time (5, 10, 15, and 20 h). Then, all AWs were fixed with 2.5% glutaraldehyde for 1 h at room temperature. After washing the samples with PBS three times, the samples were dehydrated through a graded series of alcohol concentrations (30%, 50%, 70%, 80%, 90%, and 100%), with each concentration being sustained for 15 min. Finally, the adhesion of the *S. mutans* on the AWs was examined by SEM and counted by ImageJ. The bacteria were distinguished from the underlying surfaces of AWs according to their inherent size and morphology (Figure S7, Supporting Information).^[30]

Durability of Hydrophobicity of FAS-AWs: To verify the durability of the FAS-AWs, the static contact angles of the FAS-AWs were measured after incubating them in the bacterial suspension for different times. First, the FAS-AWs were immersed into the bacterial suspension for 20 h and then removed every 5 h. To exclude the effect of the adhesive bacteria, the FAS-AWs were all ultrasonicated in deionized water for approximately 30 min. Finally, the stable contact angles revealed the durability of the hydrophobicity of the FAS-AWs.

Anti-Ni Release Performance of AWs: To evaluate the anti-Ni release performance, four representative AWs were immersed in the bacterial suspension for 5 h, including Bare-LAW, Bare-HAW, FAS-LAW, and FAS-HAW. Then, after all AWs were removed, the remaining bacterial suspension was centrifuged at 2000 rpm for 10 min, and the supernatant was collected for ICP-MS to detect nickel concentration.

Electrochemical Corrosion Resistance of FAS-AWs: The anti-electrochemical corrosion capability of the AWs before and after FAS modification was studied by potentiodynamic polarization experiments. The as-prepared AWs were dipped into the electrolyte (normal saline) of the three-electrode system, and the potential was scanned from -1000 to $+1000$ mV at a scan rate of 5 mV s^{-1} . The corrosion potential and the corrosion current density of the as-prepared Ni–Ti alloys were measured by the method of Tafel plot extrapolation.

Mechanical Properties Measurement: Flexural strength was investigated in a three-point bending test.^[28] The Bare-LAWs (Control) and FAS-AWs with different roughness were tested using a universal testing machine according to ISO/CD 15841:2004, MOD standard (short side of the cross-section was selected as the driving face, with fulcrum distance 10 mm and loading rate 1 mm min^{-1} , under temperature of $36 \pm 1 \text{ }^\circ\text{C}$) and a stress–strain curve was drawn to visualize the flexural properties.

Supporting Information

Supporting Information is available from the Wiley Online Library or from the author.

Acknowledgements

R.L. and X.L. contributed equally to this work. This research was supported by the National Key R&D Program of Ministry of Science and Technology of China (Grant No. 2018YFC1105301), the National Research Fund for the National Natural Science Foundation of China (Grant Nos. 51173004, 21875269, 21501184, and 21425314), the National Program for the National Program for Special Support of Eminent Professionals of Organization Department of the CPC Central Committee, and the Youth Innovation Promotion Association CAS (Grant No. 2017036).

Conflict of Interest

The authors declare no conflict of interest.

Keywords

antibacteria adhesion, anti-Ni ion release, bioinspired, Ni–Ti alloy archwires, superhydrophobic surface

Received: October 8, 2018

Revised: January 9, 2019

Published online: January 25, 2019

- [1] H. M. Chen, W. Z. Zhang, G. Z. Zhu, J. Xie, X. Y. Chen, *Nat. Rev. Mater.* **2017**, 2, 17024.
 [2] a) J. Xue, J. W. Xie, W. Y. Liu, Y. N. Xia, *Acc. Chem. Res.* **2017**, 50, 1976; b) Y. Q. Zhang, M. H. Wu, X. Han, P. Wang, L. D. Qin, *Angew. Chem., Int. Ed.* **2015**, 54, 10838.
 [3] a) B. Yu, S. Y. Kang, A. Akthakul, N. Ramadurai, M. Pilkenton, A. Patel, A. Nashat, D. G. Anderson, F. H. Sakamoto, B. A. Gilchrist, R. R. Anderson, R. Langer, *Nat. Mater.* **2016**, 15, 911; b) M. Williams, J. Jezior, *Nat. Rev. Urol.* **2013**, 10, 504.
 [4] a) S. A. Castleberry, B. D. Almquist, W. Li, T. Reis, J. Chow, S. Mayner, P. T. Hammond, *Adv. Mater.* **2016**, 28, 1809; b) M. D. Konieczynska, M. W. Grinstaff, *Acc. Chem. Res.* **2017**, 50, 151; c) W. W. Xu, Q. A. Song, J. F. Xu, M. J. Serpe, X. Zhang, *ACS Appl. Mater. Interfaces* **2017**, 9, 11368.

- [5] W. J. Buehler, R. C. Wiley, J. V. Gilfrich, *J. Appl. Phys.* **1963**, 34, 1475.
 [6] S. P. Humphrey, R. T. Williamson, *J. Prosthet. Dent.* **2001**, 85, 162.
 [7] C. J. Hwang, J. S. Shin, J. Y. Cha, *Am. J. Orthod. Dentofacial Orthop.* **2001**, 120, 383.
 [8] a) W. G. Koh, A. Revzin, A. Simonian, T. Reeves, M. Pishko, *Biomed. Microdevices* **2003**, 5, 11; b) L. Y. Peng, L. Chang, X. Liu, J. X. Lin, H. L. Liu, B. Han, S. T. Wang, *ACS Appl. Mater. Interfaces* **2017**, 9, 17688.
 [9] a) G. Cheng, Z. Zhang, S. F. Chen, J. D. Bryers, S. Y. Jiang, *Biomaterials* **2007**, 28, 4192; b) Z. Q. Cao, L. Mi, J. Mendiola, J. R. Ella-Menye, L. Zhang, H. Xue, S. Y. Jiang, *Angew. Chem., Int. Ed.* **2012**, 51, 2602.
 [10] a) S. M. Olsen, L. T. Pedersen, M. H. Laursen, S. Kiil, K. Dam-Johansen, *Biofouling* **2007**, 23, 369; b) J. J. T. M. Swartjes, T. Das, S. Sharifi, G. Subbiahdoss, P. K. Sharma, B. P. Krom, H. J. Busscher, H. C. van der Mei, *Adv. Funct. Mater.* **2013**, 23, 2843.
 [11] a) Y. H. An, G. W. Stuart, S. J. McDowell, S. E. McDaniel, Q. Kang, R. J. Friedman, *J. Orthop. Res.* **1996**, 14, 846; b) X. Liu, L. Y. Peng, J. X. Meng, Z. P. Zhu, B. Han, S. T. Wang, *Nanoscale* **2018**, 10, 2711.
 [12] H. W. Wang, L. Wang, P. C. Zhang, L. Yuan, Q. A. Yu, H. Chen, *Colloids Surf., B* **2011**, 83, 355.
 [13] S. Chernousova, M. Epple, *Angew. Chem., Int. Ed.* **2013**, 52, 1636.
 [14] a) E. I. Rabea, M. E. T. Badawy, C. V. Stevens, G. Smaggha, W. Steurbaut, *Biomacromolecules* **2003**, 4, 1457; b) P. Sahariah, V. S. Gaware, R. Lieder, S. Jonsdottir, M. A. Hjalmarsdottir, O. E. Sigurjonsson, M. Masson, *Mar. Drugs* **2014**, 12, 4635.
 [15] E. Ostorhazi, M. C. Holub, R. Ferenc, H. Ferenc, M. Cassone, J. D. Wade, L. Otvos, *Int. J. Antimicrob. Agents* **2011**, 37, 480.
 [16] a) K. Manabe, S. Nishizawa, S. Shiratori, *ACS Appl. Mater. Interfaces* **2013**, 5, 11900; b) X. L. Li, *Phys. Chem. Chem. Phys.* **2016**, 18, 1311; c) K. Nowlin, A. Boseman, A. Covell, D. LaJeunesse, *J. R. Soc., Interface.* **2015**, 12, 20140999; d) C. Sengstock, M. Lopian, Y. Motemani, A. Borgmann, C. Khare, P. J. Buenconsejo, T. A. Schildhauer, A. Ludwig, M. Koller, *Nanotechnology* **2014**, 25, 195101; e) J. Hasan, S. Raj, L. Yadav, K. Chatterjee, *RSC Adv.* **2015**, 5, 44953.
 [17] a) B. Fang, Y. Jiang, V. M. Rotello, K. Nusslein, M. M. Santore, *ACS Nano* **2014**, 8, 1180; b) Q. Yu, P. Shivapooja, L. M. Johnson, G. Tizazu, G. J. Leggett, G. P. Lopez, *Nanoscale* **2013**, 5, 3632; c) Q. Yu, L. K. Ista, G. P. Lopez, *Nanoscale* **2014**, 6, 4750.
 [18] a) C. L. Chu, C. Y. Chung, P. K. Chu, *Mater. Sci. Eng., A* **2006**, 417, 104; b) C. L. Chu, T. Hu, S. L. Wu, Y. S. Dong, L. H. Yin, Y. P. Pu, P. H. Lin, C. Y. Chung, K. W. K. Yeung, P. K. Chu, *Acta Biomater.* **2007**, 3, 795; c) S. D. Plant, D. M. Grant, L. Leach, *Biomaterials* **2005**, 26, 5359.
 [19] a) M. Krishnan, S. Seema, A. V. Kumar, N. P. Varthini, K. Sukumaran, V. R. Pawar, V. Arora, *Angle Orthod.* **2014**, 84, 358; b) T. R. Tripi, A. Bonaccorso, G. G. Condorelli, *J. Endod.* **2003**, 29, 132.
 [20] H. C. Man, K. L. Ho, Z. D. Cui, *Surf. Coat. Technol.* **2006**, 200, 4612.
 [21] a) K. W. K. Yeung, R. W. Y. Poon, X. Y. Liu, J. P. Y. Ho, C. Y. Chung, P. K. Chu, W. W. Lu, D. Chan, K. M. C. Cheung, *J. Biomed. Mater. Res., Part A* **2005**, 75a, 256; b) C. Ohkubo, I. Shimura, T. Aoki, S. Hanatani, T. Hosoi, M. Hattori, Y. Oda, T. Okabe, *Biomaterials* **2003**, 24, 3377.
 [22] S. Shabalovskaya, J. Andereg, J. Van Humbeeck, *Acta Biomater.* **2008**, 4, 447.
 [23] a) M. J. Liu, S. T. Wang, L. Jiang, *Nat. Rev. Mater.* **2017**, 2, 17036; b) B. Su, Y. Tian, L. Jiang, *J. Am. Chem. Soc.* **2016**, 138, 1727.
 [24] a) M. J. Kreder, J. Alvarenga, P. Kim, J. Aizenberg, *Nat. Rev. Mater.* **2016**, 1, 15003; b) L. Mishchenko, B. Hatton, V. Bahadur, J. A. Taylor, T. Krupenkin, J. Aizenberg, *ACS Nano* **2010**, 4, 7699.
 [25] a) Y. F. Li, J. H. Zhang, S. J. Zhu, H. P. Dong, Z. H. Wang, Z. Q. Sun, J. R. Guo, B. Yang, *J. Mater. Chem.* **2009**, 19, 1806; b) X. F. Gao, X. Yan, X. Yao, L. Xu, K. Zhang, J. H. Zhang, B. Yang, L. Jiang, *Adv. Mater.* **2007**, 19, 2213.

- [26] a) S. J. Gao, J. C. Sun, P. P. Liu, F. Zhang, W. B. Zhang, S. L. Yuan, J. Y. Li, J. Jin, *Adv. Mater.* **2016**, *28*, 5307; b) L. Wang, Y. Zhao, Y. Tian, L. Jiang, *Angew. Chem., Int. Ed.* **2015**, *54*, 14732; c) Z. X. Xue, S. T. Wang, L. Lin, L. Chen, M. J. Liu, L. Feng, L. Jiang, *Adv. Mater.* **2011**, *23*, 4270.
- [27] a) P. C. Zhang, L. Lin, D. M. Zang, X. L. Guo, M. J. Liu, *Small* **2017**, *13*, 1; b) D. M. Zang, H. Yi, Z. D. Gu, L. Chen, D. Han, X. L. Guo, S. T. Wang, M. J. Liu, L. Jiang, *Adv. Mater.* **2017**, *29*, 1602869;
- c) X. Q. Dou, D. Zhang, C. L. Feng, L. Jiang, *ACS Nano* **2015**, *9*, 10664; d) C. H. Xue, J. Chen, W. Yin, S. T. Jia, J. Z. Ma, *Appl. Surf. Sci.* **2012**, *258*, 2468.
- [28] H. Bellini, J. Moyano, J. Gil, A. Puigdollers, *J. Mater. Sci.: Mater. Med.* **2016**, *27*, 158.
- [29] T. Larsen, N. E. Fiehn, *APMIS* **2017**, *125*, 376.
- [30] L. Samaranayake, *Essential Microbiology for Dentistry*, Churchill Livingstone, New York **1996**, p. 73.